

Available online at www.sciencedirect.com

jmr&t
Journal of Materials Research and Technology
www.jmrt.com.br



Original Article

Tool material effect on the friction stir butt welding of AA2124-T4 Alloy Matrix MMC

Yahya Bozkurt^{a,*}, Zakaria Boumerzoug^b

^a Marmara University, Faculty of Technology, Department of Metallurgy and Materials Engineering, Goztepe Campus, 34722 Kadıkoy-Istanbul, Turkey

^b Department of Mechanical Engineering, LMSM, University of Biskra, B.P.145, Biskra 07000, Algeria

ARTICLE INFO

Article history:

Received 6 March 2017

Accepted 4 April 2017

Available online xxx

Keywords:

Friction stir welding

AA2124-T4 alloy matrix MMC

Tool wear

Tensile test

ABSTRACT

The purpose of the present work is to study on the effect of material properties tool on friction stir butt welding of AA2124-T4 alloy matrix MMC. Uncoated tool, coated tool with a CrN, and coated tool with AlTiN were used to weld aluminum MMC plates. Macrostructure and microstructure observations, ultimate tensile strength, wear resistance, and chemical analysis were carried out to determine the appropriate tool for joining these composite plates. Results showed that the good welded joints could be obtained when a tool is coated with AlTiN.

© 2017 Brazilian Metallurgical, Materials and Mining Association. Published by Elsevier Editora Ltda. This is an open access article under the CC BY-NC-ND license (<http://creativecommons.org/licenses/by-nc-nd/4.0/>).

1. Introduction

Aluminum based metal matrix composites (AlMMCs) are considered as one of the most encouraging structural materials for contemporary engineering applications in fields of aeronautical, military, and automotive industries [1]. They possess an improved specific stiffness and strength to weight ratio at room and elevated temperatures, superior wear resistance, fatigue properties and formability, and greater thermal stability in respect to the corresponding unreinforced matrix alloys [2,3].

In order to construct a large and complex structural component, sometimes it is necessary to join aluminum composites

to themselves or to other materials. However, joining of aluminum composites using conventional methods is a difficult task due to the presence of reinforced particles [1]. Friction stir welding (FSW) has emerged as a promising technique for joining of MMCs. In this process, joining is applied at temperatures below the melting point of the base material and therefore the solidification micro-structure is absent in the weld like dendrite structure and the undesirable particle-matrix interface reactions is also eliminated [4-6].

FSW is widely used as green welding process which is widely adopted in different industries including the aerospace, automotive and manufacturing industry field joining aluminum alloy composite that are hard to weld by fusion welding process [7]. FSW can be performed on a variety

* Corresponding author.

E-mail: ybozkurt@marmara.edu.tr (Y. Bozkurt).

<http://dx.doi.org/10.1016/j.jmrt.2017.04.001>

2238-7854/© 2017 Brazilian Metallurgical, Materials and Mining Association. Published by Elsevier Editora Ltda. This is an open access article under the CC BY-NC-ND license (<http://creativecommons.org/licenses/by-nc-nd/4.0/>).

of joint configurations including butt joint, lap joint and T joint [4]. Friction stir butt welding utilizes a non-consumable rotating tool with a specially designed shoulder and profiled probe that is plunged into the interface between two plates to be joined and traversed along the line of joint. But, during FSW localized frictional heat is generated between the tool shoulder and work piece top surface. Plastic deformation heat is also generated due to mechanical stirring of the probe. Frictional heating by tool shoulder and stirring action of the probe produce highly plastically deformed weld nugget zone [8–10]. Four distinct regions in the weldment are: nugget zone (NZ), thermo-mechanically affected zone (TMAZ), heat-affected zone (HAZ) and the base material (BM) [2,11,12]. The severe heating of the tool has been noticed during FSW, and in addition to this it has been observed that important wear may develop if the tool material has low yield strength at high temperatures. Stresses applied by the tool depend on the strength of the work piece at high temperatures are common under the FSW conditions. In addition, temperatures in the work piece depend on the material properties of tool such as thermal conductivity [13].

The applicability of FSW to join aluminum MMCs reinforced with ceramic particles has been investigated by several authors [14–16]. Fernandez and Murr [17] studied the FSW of cast Al-359/20% SiC composite. They focused on the effect of FSW tool rotational speed and weld speed for reducing the tool wear rate. The results indicated that the minimum wear obtained with the lowest tool rotation speed. Bozkurt et al. [14] investigated the FSW of AA2124/SiC/25p-T4 composite plates and noted a decrease up to 19% in tensile strength and 58% in ductility as compared to the base material. In other investigation, Bozkurt has investigated weldability of same MMC plates at low welding speed. He has observed that grain size changes from base MMC to stir zone. Fracture surfaces have revealed a mixed brittle-ductile mode, due to age hardening mechanism the increase in hardness from both advancing and retreating side of the HAZ to TMAZ [5]. Prater [18] characterized the tool wear in FSW of A359/20% SiC MMCs by varying process parameters. It was also observed that with increase in the welding speed, the ultimate tensile strength (UTS) of the joints decreased [19]. Mishra and Ma [8] addressed that tool wear and shape optimization are associated with the tool materials and further research is needed for selection of tool material.

As it has been reported, a production of a quality FSW needs a selection of the appropriate tool material for a specific application. Thus, it is unsuitable to have a tool that loses dimensional stability, the designed features, or fractures [20]. The following parameters and characteristics have to be considered for material selection: ambient and elevated temperature strength, elevated temperature stability, wear resistance, tool reactivity, fracture toughness, coefficient of thermal expansion, machinability [13]. There are number of criteria included for the tool material selection. Although, different researchers have selected the tool material based on literature, experience or conjectural but this does not precise the optimum tool material selection. Padmanaban and Balasubramanian [21] used to fabricate the joints five different tool materials such as mild steel, stainless steel, armor steel, high carbon steel and high speed steel (HSS). They have not

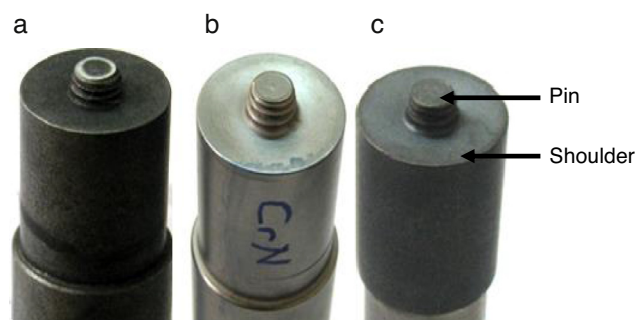


Fig. 1 – Tools of FSWed of MMC plates: (a) Uncoated tool, (b) CrN coated tool, (c) AlTiN coated tool.

proposed any procedure to select a tool material. They reported that using HSS and high carbon steel as a tool material defect free nugget zone and high tensile properties.

The objective of this present work is to study the tool effect on friction stir butt welding of AA2124-T4 alloy matrix MMC. The base material of the FSW tool was a HSS. Three different tools were chosen, i.e., uncoated tool, coated tool with a CrN, and coated tool with a AlTiN were used to weld aluminum MMC plates.

2. Experimental procedures

The plates used in this study are AA2124-T4 alloy matrix MMC strengthened with 25% SiC particles (AA2124/SiC/25p-T4). This material was supplied by Aerospace Metal Composite Limited (UK) in form of billet with size of 400 × 260 × 50 mm. The MMC material was produced by powder metallurgy and mechanical alloying techniques followed by hot forging and tempering to T4 condition (solution heating at about 505 °C for 1 h, quenching in 25% polymer glycol solution and room temperature aging for >100 h). The chemical composition of the AA2124/SiC/25p-T4 MMC is presented in Table 1. The main mechanical properties are presented in Table 2. As it is indicated in Table 2, the UTS of the base AA2124/SiC/25p-T4 MMC is of 454 MPa. MMC plates of 130 × 50 × 3 mm size were cut from this billet by electro-discharge machining (EDM) technique with a feeding rate of 2 mm/min.

The AA2124/SiC/25p-T4 MMC plates were friction stir butt welded using an FSW adapted numeric controlled milling machine. The FSW tool was of HSS with shoulder and probe (pin) diameter 18 and 6 mm, respectively. The tool was tilted by 2° with respect to Z-axis of milling machine and rotated in clockwise direction chosen according to the optimum results. FSW process was carried out at the tool rotation speed of 900 rpm and tool traverse speed of 45 and 115 mm/min. The FSW tool was a HSS. The microhardness of the tools was measured using a digital computerized Shimadzu microhardness tester with a load of 1.9 g for a duration of 30 s. For this investigation, the three different FSW tools were used (Fig. 1); uncoated tool, coated with a CrN, and coated with a AlTiN. The different stages of FSW process are presented in Fig. 2.

The tensile tests were also carried out at room temperature according to ISO/TTA2 standard [22] using universal type tensile test machine Zwick Z010 to determine the tensile

Table 1 – Chemical composition of AA2124/SiCp/25-T4 MMC plates.

Materials	Chemical composition (% mass)				
	Cu	Mg	Mn	Si	Al
AA2124/SiCp/25-T4	3.86	1.52	0.65	0.17	93.8

Table 2 – Mechanical properties of AA2124/SiCp/25-T4 MMC plates.

Materials	Ultimate tensile strength (MPa)	Yield Strength (MPa)	% Elongation	Hardness (HV)
AA2124/SiCp/25-T4	454	390	1.38	190

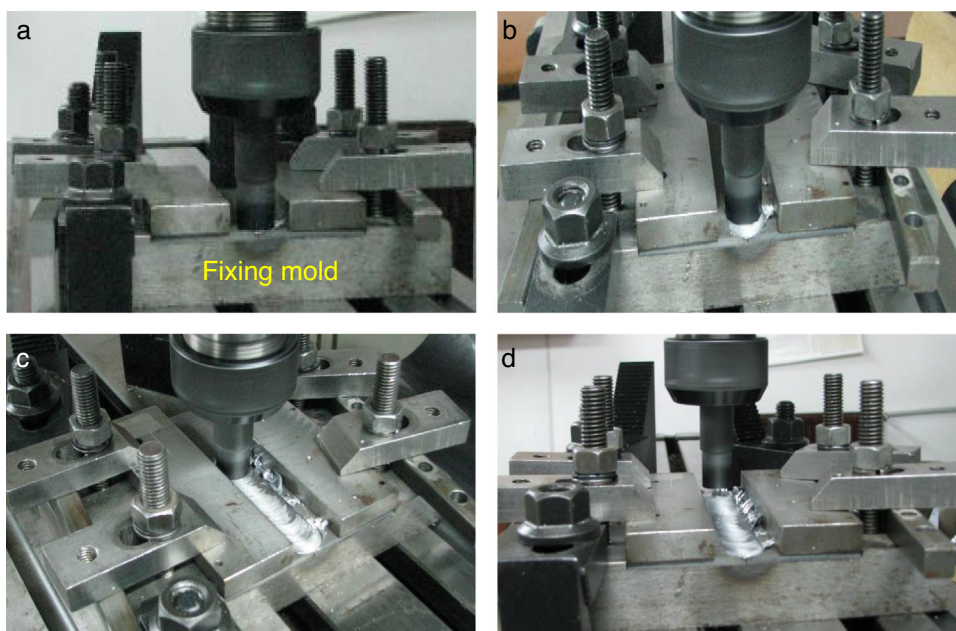


Fig. 2 – Stages of FSW Process: (a) rotating tool prior to penetration into the butt joint; (b) tool shoulder makes contact with the part, creating heat; (c) restricting further penetration while expanding the hot zone and moving parts under the tool, creating a friction stir weld nugget; (d) retraction of the tool from the joining zone.

properties of the joints. Three specimens were tested under the same conditions to guarantee the reliability of the results. Microstructural and chemical analyses were performed from the cross-sections of FSWed joints by scanning electron microscope (SEM) Jeol JSM-5910 LV. The distributions of chemical elements in the fractured zone were performed by energy dispersive X-ray spectroscopy (EDS) system.

3. Results and discussions

3.1. Surface appearance

Fig. 3 shows the top and bottom surfaces after FSW of MMCs plates with three different tools. As shown in Fig. 1, AA2124-T4 Alloy Matrix MMC plates were successfully joined by FSW technique. From the visual examinations of the top view of the FSWed composites, the flash effect was produced on the top surface of weld made by three tools. This kind of defect is more apparent in welded joint by uncoated (Fig. 3a) and CrN coated tool (Fig. 3b) than welded aluminum MMC plates by AlTiN coated tool (Fig. 3c). This flash effect was due to the

hot condition in which the material was highly deformed and extruded out-side [23,24]. On the other hand, no visible shallow porosity or other macroscopic defects have been observed in bottom view of welded AA2124-T4 alloy matrix MMC joints. In addition, if the pin is not long enough or the tool rises out of the plate then the interface at the bottom of the weld is disrupted and forged by the tool, resulting in a lack-of-penetration defect. This is essentially a notch in the material, which is a potential source of fatigue cracks [25]. As shown in Fig. 3 appearances of the bottom view, shoulder and pin show that penetrate deeply enough and sufficient penetration.

3.2. Wear resistance

It is known that a weld quality and tool wear are two important considerations in the selection of tool material. Significant tool wear increases the processing cost of FSW [13]. Tool wear during welding of MMCs is greater when compared with welding of mild alloys due to the presence of hard, abrasive phases in the composites [26]. For FSW of AlMMCs, some studies [17,27,28] have shown that the tool wears initially and obtains

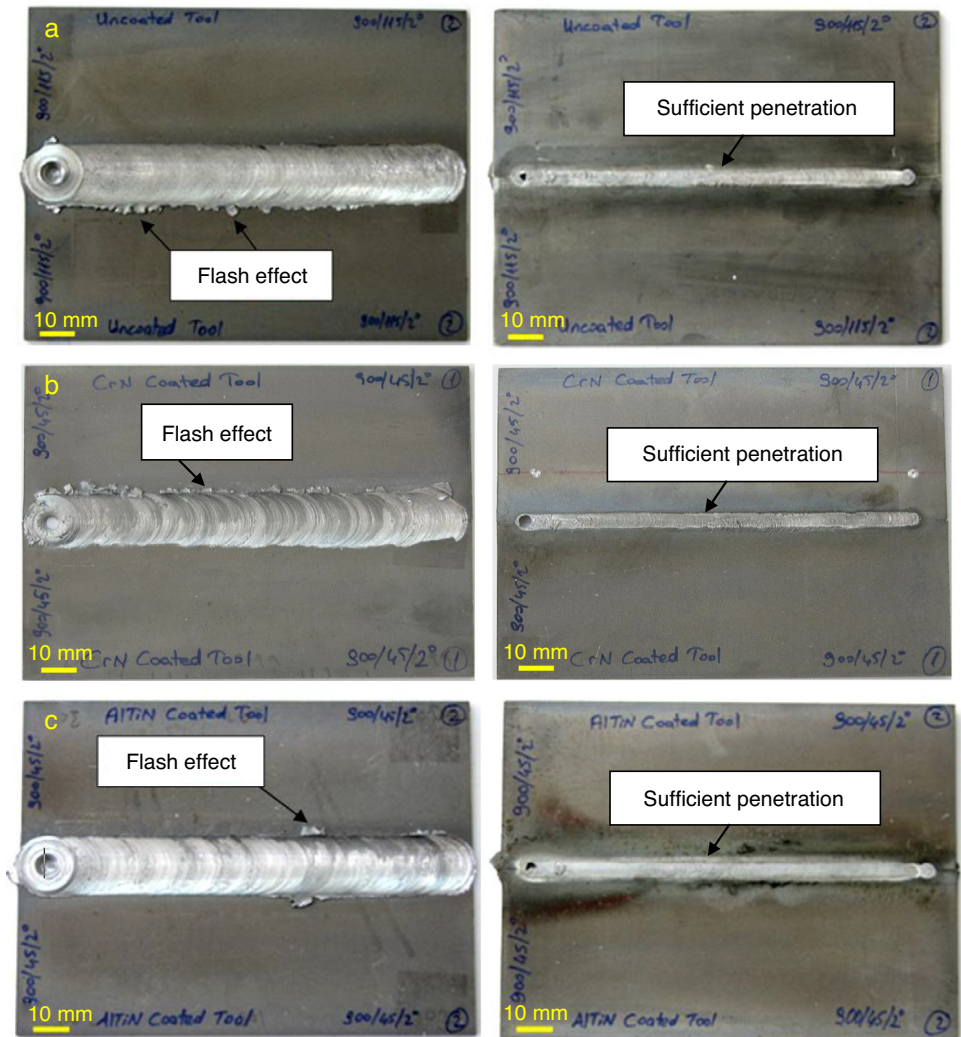


Fig. 3 – Appearances of top and bottom view after FSW: (a) Uncoated tool, (b) CrN coated tool, (c) AlTiN coated tool.

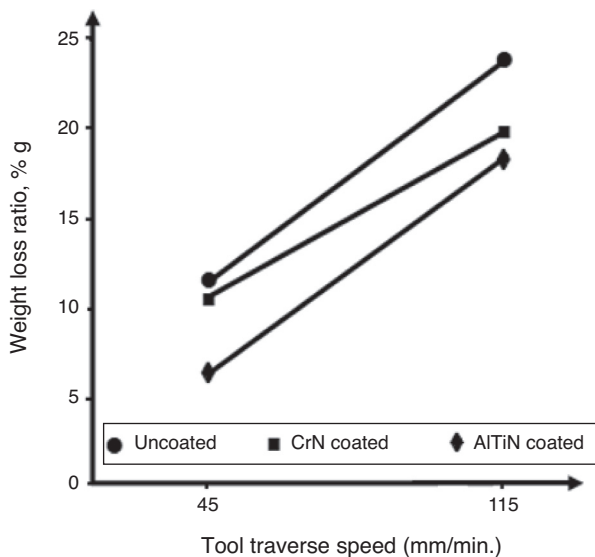


Fig. 4 – Effect of tool traverse speed on weight loss ratio.

a self-optimized shape after which wear becomes much less pronounced [26].

Fig. 4 shows the variations in weight loss ratio of tool. It is obvious that the weight loss ratio increases with increasing tool traverse speed but the coated tool with AlTiN has the lowest weight loss ratio. This result indicates that deposited

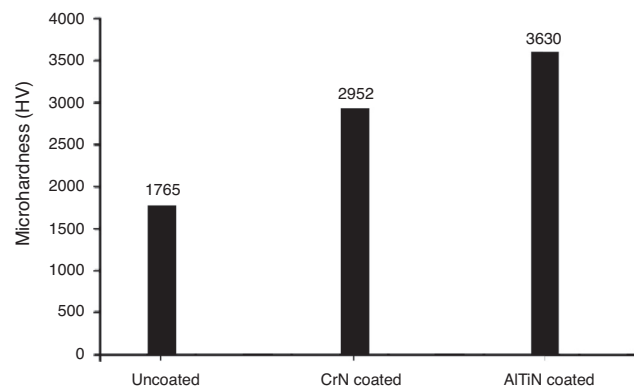


Fig. 5 – Microhardness values for three tools.



Fig. 6 – Macrographic views of: (a) uncoated tool, (b) CrN coated tool, (c) AlTiN coated tool before and after welding process.

AlTiN film has a high wear resistance. It has been found that many wear resistant coatings show high hardness [29]. The hardness values for these three tools are given in Fig. 5. In our case, the highest hardness value was obtained for the AlTiN coated tool. This high wear resistance is due to highest value of hardness of the coated tool with AlTiN (3630 HV).

Visual examinations of before and after welding process are shown in Fig. 6. The tool pin lost its original geometry. The shoulder size and pin length are changed slightly and the radial wear of the pin is most severe for the whole tools. This indicates that the radial wear of the pin is unequal at different locations of the pin. It has been found that the tool wear,

deformation and failure are also much more remarkable in the tool pin compared with the tool shoulder [25]. We notice that a limited investigations in the literature reported that tool wear occurs during FSW of Al matrix ceramic particulate-reinforced composites [2,14,17,30]. For example, Cioffi et al. [31], used MP159 and H13 as tool material for threaded pin and shoulder, respectively. At a rotation speed of 800 rpm, intense wear of the pin occurred in welding 15 mm thick AA2124/SiC/25p plates. Recently, Prater et al. [18], compared wear resistance among different types of tool materials including O1 steel, Wc-Co micron, Wc-Co submicron, and Wc-Co coated by diamond to weld AA359/SiC/20p-T6 and AA359/SiC/30p-T6. They found

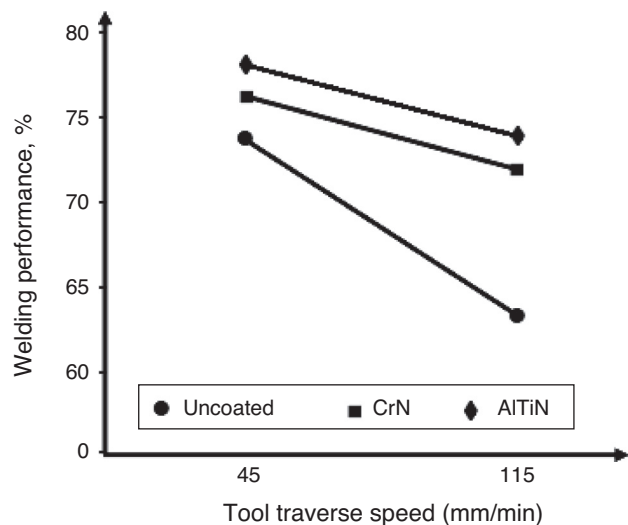


Fig. 7 – Welding performance with tool traverse speed.

that harder material can be used to decrease the wear of tool by 60–80%. However, the toughness of the tool is another parameter which causes tool fracture in FSW. Consequently, surface coating can be used to minimize the abrasive wear in the FSW tool [14,32].

The wear rate is maximum in three tools when FSWed by 900/115 welding parameters. Weight loss ratio is 0.235 g, 0.190 g and 0.174 g in uncoated, CrN coated and AlTiN coated tool, respectively. Therefore, severe wear occurs when uncoated tool is used as tool material. It was obtained minimum wear in AlTiN coated tool by 900/45 welding parameters. The vortex flow of uncoated tool is lesser than the AlTiN coated tool due to the abraded (eroded) threads as shown in Fig. 5.

3.3. Tensile test results

The tensile test results for the FSWed joints made after CCT are given in Table 3. These UTS values of welded joint were obtained after using three different tools with varying the tool traverse speed (45 and 115 mm/min). It is seen from this table that the maximum UTS values were obtained by using AlTiN coated tool. In addition, the increase of the tool traverse speed decreases the UTS values and welding performance for all the three tools as shown in Table 3 and Fig. 7, respectively.

During the FSW, the material in the weld undergoes intense plastic deformation at elevated temperature, but it is not melted because of self-adaption behavior [33]. The temperature reduction occurring in the volume space causes rapid cooling of the stir zone. Therefore, this rapid cooling was increased abrasion resistance and decreased UTS. Obviously, AlTiN coated tool plays a significant influence

on joint quality during FSW. It is seen that the tensile strength of the joint reach the maximum values of 355.15 MPa and the welding performance value greater than 78% (i.e., $UTS_{FSW}/UTS_{BaseMMC} \times 100$). It is evident that there is a direct relation between tool traverse speed and welding performance as shown in Fig. 7. Similar results were also obtained by some researchers [34] for the FSWed AA2219-T87 age hardenable aluminum-copper alloys and AA6061/20% Al_2O_3 p MMC plates. These results demonstrate that the FSW is highly effective for mechanical property improvements resulting from grain refinement.

Meanwhile, the mechanical properties of the joint under the uncoated tool are minimum. In fact, the joint quality is closely related to softening of the joint and defect location [35]. Fig. 8 exhibits fracture location of joints using AlTiN coated (Fig. 8a) and uncoated (Fig. 8b) tools with 900/45 and 900/115 welding parameters after tensile test, respectively. It is well known that the fracture in MMCs is controlled by three main mechanisms: (1) cracking of the reinforcing particles, (2) interfacial decohesion at the particle-matrix interface resulting in the nucleation of voids, and (3) growth and coalescence of voids in the matrix. Accordingly, the fracture surfaces of tensile specimens are usually described by a bimodal distribution of large voids, associated with the particle reinforcement [14]. For the base metal, an increased concentration of SiC particles increases the strength and decreases the elongation to failure of the MMC.

During the tensile tests, two different failure locations were reported: in the NZ and in the TMAZ. FSWed by AlTiN coated tool specimens failed in the TMAZ (Fig. 8a), because of SiC particulates probably non-uniform distributed in this zone. When the fracture occurs in the TMAZ, it is always located on the advancing side of the weld as shown in Fig. 8a. The fractures observed in the NZ are mainly due to localized defects such as root flaws, lack of penetration and metal particles broken from the uncoated tool (Fig. 8b).

3.4. SEM and EDS analysis

In this part we present just the analysis by SEM and EDS of welded joint by uncoated and AlTiN coated tool, respectively.

A better comprehension and understanding of the mechanical fracture and defect nucleation properties depend on purposed analyses of the fracture surfaces, since the influence of microstructural morphology of the joined interfaces on the endurance time results to be fundamental [36]. Figs. 9 and 10 show both fracture surfaces after tensile test and EDS analysis of welded joint with welding parameters 900/115 and 900/45 of uncoated and AlTiN coated tool, respectively. In the first joint (Fig. 9), the fracture surfaces revealed a mixed brittle-ductile fracture mode. Different particles with different dimension and mode were observed in fractured surface.

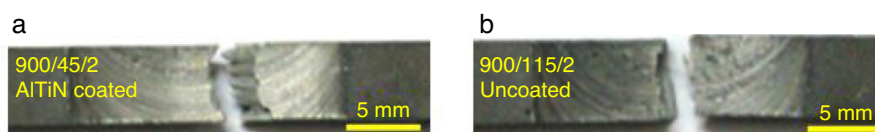
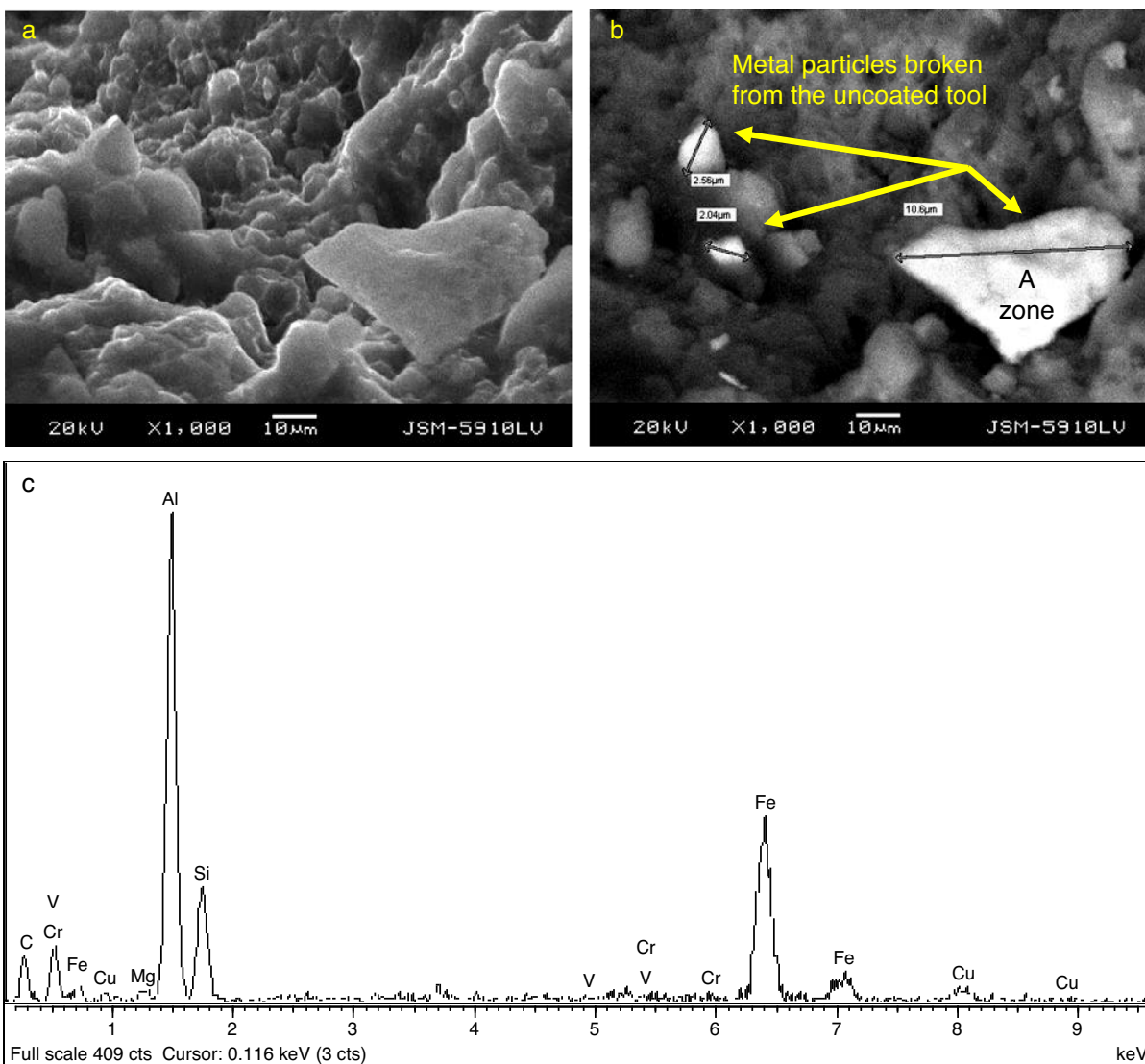


Fig. 8 – Position of the fracture after tensile test of welded of MMCs plates: (a) 900/45 and (b) 900/115.

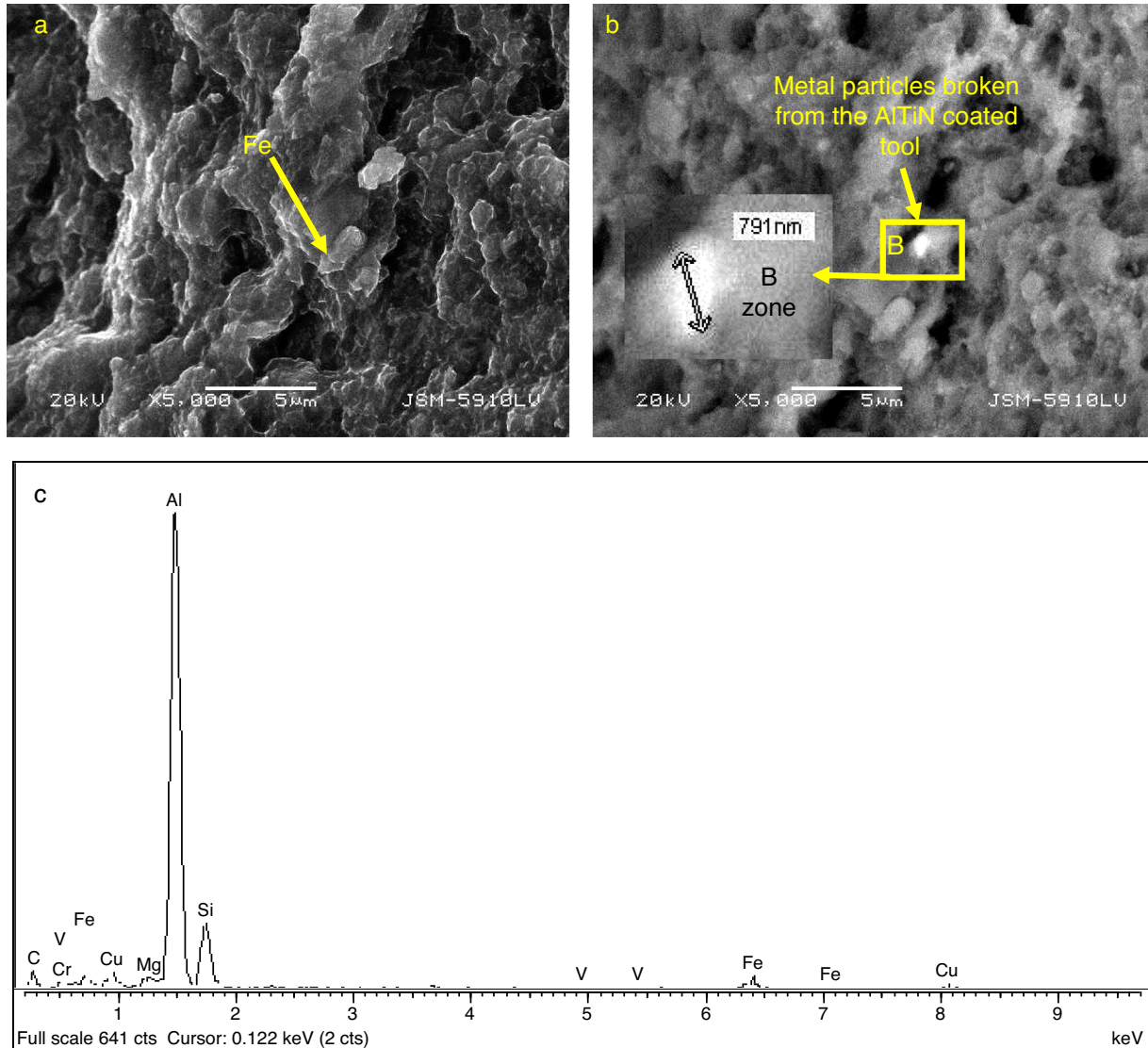
Table 3 – The tensile test results for the FSWed joints.

Tool	Tool rotation speed (rpm/min)	Tool traverse speed (mm/min)	Tool tilt angle (°)	UTS (MPa)
Uncoated	900	45	2	331.70
		115		288.12
CrN coated	900	45	2	346.32
		115		328.30
AlTiN coated	900	45	2	355.15
		115		335.98



Welding parameters and zone	Chemical element, %								
	C	Mg	Al	Si	V	Cr	Fe	Cu	Toplam
900/115 A zone	30.06	0.52	24.99	7.73	0.31	0.34	31.87	4.18	100.00

Fig. 9 – (a) SEM, (b) BEI (backscattered electron image) and (c) EDS analysis of the fracture surface after tensile test of welded joint by uncoated tool (900/115 welding parameters).



Welding parameters and zone	Chemical element,%								
	C	Mg	Al	Si	V	Cr	Fe	Cu	Toplam
900/45 B zone	34.10	0.95	46.35	11.77	0.02	0.60	3.90	2.31	100.00

Fig. 10 – (a) SEM, (b) BEI (backscattered electron image) and (c) EDS analysis of the fracture surface after tensile test of welded joint by AlTiN coated tool (900/45 welding parameters).

For example, an iron particle cracking was found in the NZ (Fig. 9a and b). The EDS analysis revealed high quantity of iron (31.87%) for uncoated tool. A bright point in the BEI micrograph (Fig. 9b) is observed as 2.04 µm, 2.56 µm and 10.6 µm (A zone: greatest Fe particle) metal particles broken from the uncoated tool. Some elements like Fe, Cr, C and V were detected by EDS analysis in NZ (Fig. 9c and 10c). The presence of these elements is because of the wear of uncoated HSS steel tool. In addition, no traces of oxygen in this region were found which avoids the formation of undesirable particles like iron-oxide. However, In the case of 900/45 welding parameters joint (Fig. 10a), a ductile fracture mode appears and the EDS analysis indicates a

few quantity of iron (3.9%) (Fig. 10c), as bright point in the BEI micrograph (Fig. 10b) with size of 791 nm (B zone: Fe particle) metal particles broken from the AlTiN coated tool. Therefore, the greatest wear occurred in the uncoated tool wear. Heavy deformations in the NZ cause breaking of SiC particles.

4. Conclusion

This study focused on the material properties tool effect on friction stir butt welding of AA2124-T4 alloy matrix MMC. The obtained results can be summarized as follows:

1. The AA2124-T4 alloy matrix MMC plates were successfully joined by FSW.
2. In microstructural examination, no visible superficial porosity has been observed in AA2124-T4 alloy matrix MMC joints, but some neglected macroscopic defects have been observed.
3. The maximum UTS values of welded MMC plates were obtained by using AlTiN coated tool.
4. The joints exhibited two different fracture modes. Both a mixed brittle-ductile fracture and the comparatively ductile fracture mode were observed for both types of welds in UTS tensile tests. The welds displaying low UTS values fractured with a mixed brittle-ductile fracture, whereas a ductile fracture mode was exhibited by the joints showing higher UTS values.
5. The radial wear of the pin is very different for three tools namely, uncoated, CrN coated and AlTiN coated tool, and the maximum wear was observed at uncoated tool as 0.235 g wear loss ratio.
6. The welding speed has a certain effect on radial wear rate of the pin. The higher the welding speed, the higher the wear rate, and the maximum wear rate is observed in 900/115 welding parameters with uncoated tool.
7. EDS analysis detected Fe, Cr, C and V in NZ, which is due to the tool wear.
8. The tensile strength of the joint reach the maximum values of 355.15 MPa and the welding performance value greater than 78% by AlTiN coated tool.

Conflicts of interest

The author declares no conflicts of interest

Acknowledgement

This study was financially supported by the Marmara University Scientific Research Fund, Grant No.: FEN-C-YLP-280110-0012.

REFERENCES

- [1] Veerendra, Keshavamurthy R, Prakash CPS. Microstructure and hardness distribution in friction stir welded Al6061-TiB₂ in-situ metal matrix composite. *Int J Mech Prop Eng* 2014;2(9):73-6. IRAJ doi:IJMPE-IRAJ-DOI-1240.
- [2] Uzun H. Friction stir welding of SiC particulate reinforced AA2124 aluminium alloy matrix composite. *Mater Des* 2007;28:1440-6, <http://dx.doi.org/10.1016/j.matdes.2006.03.023>.
- [3] Rotundo F, Ceschini L, Morri A, Jun TS, Korsunsky AM. Mechanical and microstructural characterization of 2124Al/25vol%SiCp joints obtained by linear friction welding (LFW). *Composites A* 2010;41:1028-37, <http://dx.doi.org/10.1016/j.compositesa.2010.03.009>.
- [4] Mishra RS, Ma ZY. Friction stir welding and processing. *Mater Sci Eng Rep* 2005;50:1-78, <http://dx.doi.org/10.1016/j.mserep.2005.07.001>.
- [5] Bozkurt Y. Weldability of metal matrix composite plates by friction stir welding at low welding parameters. *Mater Technol* 2011;45(5):407-12.
- [6] Commin L, Dumont M, Masse JE, Barrallier L. Friction stir welding of AZ31 magnesium alloy rolled sheets: influence of processing parameters. *Acta Mater* 2009;57:326-34, <http://dx.doi.org/10.1016/j.actamat.2008.09.011>.
- [7] Arya PK. A review on friction stir welding for aluminium alloy composite. *Int J Res Appl Sci Eng Technol (IJRASET)* 2015;3(XI):324-32.
- [8] Hsu CJ, Kao PW, Ho NJ. Intermetallic-reinforced aluminum matrix composites produced in situ by friction stir processing. *Mater Lett* 2007;61:1315-8, <http://dx.doi.org/10.1016/j.matlet.2006.07.021>.
- [9] Cavaliere P, Cerri E, Marzoli L, Santos JD. Friction stir welding of ceramic particle reinforced aluminium based metal matrix composites. *Appl Compos Mater* 2004;11:247-58, <http://dx.doi.org/10.1023/B:ACMA.0000035478.71092.ec>.
- [10] Berbon PB, Bingel HW, Mishra RS, Bampton CC, Mahoney MW. Friction stir processing: a tool to homogenize nanocomposites aluminum alloys. *Scr Mater* 2001;44:61-6, [http://dx.doi.org/10.1016/S1359-6462\(00\)00578-9](http://dx.doi.org/10.1016/S1359-6462(00)00578-9).
- [11] Lockwood WD, Tomaz B, Reynolds AP. Mechanical response of friction stir welded AA2024: experiment and modelling. *Mater Sci Eng* 2002;A323:348-53, [http://dx.doi.org/10.1016/S0921-5093\(01\)01385-5](http://dx.doi.org/10.1016/S0921-5093(01)01385-5).
- [12] Bousquet E, Quintin AP, Puiggali M, Devos O, Touzet M. Relationship between microstructure, microhardness and corrosion sensitivity of an AA 2024-T3 friction stir welded joint. *Corros Sci* 2011;53:3026-34, <http://dx.doi.org/10.1016/j.corsci.2011.05.049>.
- [13] Aleem Pasha MD, Ravinder Reddy P, Laxminarayana P, Khan IA. Influence of process and tool parameters on friction stir welding-over view. *Int J App Eng Technol* 2014;4(3):54-69.
- [14] Bozkurt Y, Uzun H, Salman S. Microstructure and mechanical properties of friction stir welded particulate reinforced AA2124/SiC/25p-T4 composite. *J Compos Mater* 2011;45(21):2237-45, <http://dx.doi.org/10.1177/0021998311401067>.
- [15] Amirizad M, Kokabi AH, Gharacheh MA, Sarrafi R, Shalchi B, Azizieh M. Evaluation of microstructure and mechanical properties in friction stir welded A356 + 15% SiCp cast composite. *Mater Lett* 2006;60:565-8, <http://dx.doi.org/10.1016/j.matlet.2005.09.035>.
- [16] Ceschini L, Boromei I, Minak G, Morri A, Tarterini F. Microstructure, tensile and fatigue properties of AA6061/20 vol.%Al₂O₃p friction stir welded joints. *Compos A* 2007;38:1200-10, <http://dx.doi.org/10.1016/j.compositesa.2006.06.009>.
- [17] Fernandez GJ, Murr LE. Characterization of tool wear and weld optimization in the friction-stir welding of cast aluminum 359 + 20% SiC metal matrix composite. *Mater Charact* 2004;52:65-75, <http://dx.doi.org/10.1016/j.matchar.2004.03.004>.
- [18] Prater T. Friction stir welding of metal matrix composites for use in aerospace structures. *Acta Astronaut* 2014;93:366-73, <http://dx.doi.org/10.1016/j.actaastro.2013.07.023>.
- [19] Gopalakrishnan S, Murugan N. Prediction of tensile strength of friction stir welded aluminium matrix TiCp particulate reinforced composite. *Mater Des* 2011;32:462-7, <http://dx.doi.org/10.1016/j.matdes.2010.05.055>.
- [20] Mishra RS, Mahoney MW. Friction stir welding and processing, production processes and systems. *Mater Sci Eng Rep* 2007;6(1):6-19.
- [21] Padmanaban G, Balasubramanian V. Selection of FSW tool pin profile, shoulder diameter and material for joining AZ31B magnesium alloy-An experimental approach. *Mater Des* 2009;30:2647-56, <http://dx.doi.org/10.1016/j.matdes.2008.10.021>.
- [22] Bozkurt Y, Duman S. The effect of welding parameters on the mechanical and microstructural properties of friction stir

- welded dissimilar AA 3003-H24 and 2124/SiC/25p-T4 alloy joints. *Sci Res Essay* 2011;6(17):3702–16.
- [23] Mehta KP, Badheka VJ. A review on dissimilar friction stir welding of copper to aluminum: process, properties and variants. *Mater Manuf Proc* 2016;31(3):233–54, <http://dx.doi.org/10.1080/10426914.2015.1025971>.
- [24] Mehta KP, Badheka VJ. Effects of tool pin design on formation of defects in dissimilar friction stir welding. *Procedia Technol* 2016;23:513–8, <http://dx.doi.org/10.1016/j.protcy.2016.03.057>.
- [25] Sagar SP, Miyasaka C, Ghosh M, Tittmann BR. NDE of friction stir welds of Al alloys using high-frequency acoustic microscopy, nondestructive testing and evaluation. *Nondestruct Test Eva* 2012;27(4):375–89, <http://dx.doi.org/10.1080/10589759.2012.656638>.
- [26] Rai R, De A, Bhadeshia HKDH, DebRoy T. Review: friction stir welding tools. *Sci Technol Weld Join* 2011;16(4):325–42, <http://dx.doi.org/10.1179/1362171811Y.0000000023>.
- [27] Prado RA, Murr LE, Soto KF, McClure JC. Self-optimization in tool wear for friction-stir welding of Al6061 + 20% Al₂O₃ MMC. *Mater Sci Eng A* 2003;349(1–2):156–65, [http://dx.doi.org/10.1016/S0921-5093\(02\)00750-5](http://dx.doi.org/10.1016/S0921-5093(02)00750-5).
- [28] Shindo DJ, Rivera AR, Murr LE. Shape optimization for tool wear in the friction-stir welding of cast Al359-20% SiC MMC. *J Mater Sci* 2002;37(23):4999–5005, <http://dx.doi.org/10.1023/A:1021023329430>.
- [29] Tashev P, Kondov H, Tasheva E, Kandeva M. Study on hardness and wear resistance of layers overlaid using electrodes with nano-modified coating. *Int J Eng Appl Sci* 2015;6(4):1–6.
- [30] Prado RA, Murr LE, Shindo DJ, Soto KF. Tool wear in the friction-stir welding of aluminum alloy 6061 + 20% Al₂O₃: a preliminary study. *Scr Mater* 2001;45:75–80.
- [31] Cioffi F, Fernández R, Gesto D, Rey P, Verdera D, González-Doncel G. Friction stir welding of thick plates of aluminum alloy matrix composite with a high volume fraction of ceramic reinforcement. *Compos A Appl Sci Manuf* 2013;54:117–23, <http://dx.doi.org/10.1016/j.compositesa.2013.07.011>.
- [32] Contorno D, Faga MG, Fratini L, Settineri L, Gautier di Confiengo G. Wear analysis during friction stir processing of A359 + 20%SiC MMC. *Key Eng Mater* 2009;410-411:235–44, <http://dx.doi.org/10.4028/www.scientific.net/KEM.410-411.235>.
- [33] Threadgill PL, Leonard AJ, Shercliff HR, Withers PJ. Friction stir welding of aluminium alloys. *Int Mater Rev* 2009;54(2):49–93, <http://dx.doi.org/10.1179/174328009X411136>.
- [34] Srinivasan PB, Arora KS, Dietzel W, Pandey S, Schaper MK. Characterisation of microstructure, mechanical properties and corrosion behaviour of an AA2219 friction stir weldment. *J Alloys Compd* 2010;492(1–2):631–7, <http://dx.doi.org/10.1016/j.jallcom.2009.11.198>.
- [35] Ji SD, Meng XC, Zeng YM, Ma L, Gao SS. New technique for eliminating keyhole by active-passive filling friction stir repairing. *Mater Des* 2016;97:175–82, <http://dx.doi.org/10.1016/j.matdes.2016.02.088>.
- [36] Cavaliere P, Nobile R, Panellaa FW, Squillace A. Mechanical and microstructural behaviour of 2024-7075 aluminium alloy sheets joined by friction stir welding. *Int J Mach Tool Manuf* 2006;46(6):588–94, <http://dx.doi.org/10.1016/j.ijmachtools.2005.07.010>.